MOTION OF MITOCHONDRIA IN CULTURED CELLS QUANTIFIED BY ANALYSIS OF DIGITIZED IMAGES

IRVING SALMEEN, PANOS ZACMANIDIS, GERALD JESION, AND LEE A. FELDKAMP
Research Staff, Ford Motor Company, Dearborn, Michigan 48121

ABSTRACT Translational movements of mitochondria in cultured rat liver cells were characterized quantitatively by using a video camera to detect and a video digitizer-computer system to analyze fluorescent images of mitochondria stained with rhodamine 123. The centroids of the images of individual mitochondria were determined at selected time intervals and the paths followed by the mitochondria were defined by the paths of the centroids. The predominant translational motion of the mitochondria satisfied the formal conditions of a Brownian random walk for a free particle, although in several cases there was a slow drift superimposed on the random motion. The apparent diffusion coefficients were $\sim 5 \times 10^{-12}$ cm^2 s^{-1}, and the drift speeds $\sim 2 \times 10^{-3}$ μm s^{-1}.

INTRODUCTION

Mitochondria within living cells change shape and position in times of the order of minutes. Although these movements were first observed in detail in the early 1950s by using time lapse photography of cultured cells viewed with phase contrast optics, the movements have not been quantitatively characterized and the driving forces of and constraints on the motion have not been extensively studied (1–3). A quantitative description of the motion should reveal the relative contributions of random, uniform, and periodic motion. The corresponding parameters of the motion—mean square displacement per second, frequency, and velocity, respectively—should provide the means for quantitatively testing models for the driving forces and constraints on the motion. The characterization of mitochondrial movements may also complement information obtained from the study of the motion of microinjected proteins (4) and polystyrene spheres (5).

Herein we describe measurements that lead to a quantitative characterization of the translational motion of mitochondria in cultured cells derived from rat liver. These measurements were made possible by the use of the following: staining of the mitochondria with the fluorescent dye, rhodamine 123; a silicon intensified target (SIT) video camera for detection of low intensity images at the output of a fluorescence microscope; a digital image processor for digitizing the video camera output; and computer processing of the digitized images. Rhodamine 123 stains only mitochondria and the unbound dye can be washed from the cells so as to leave no detectable background fluorescence. Therefore, the mitochondria can be detected without ambiguity or interferences. Rhodamine 123 appears to have no adverse effects on cell structure or function (6). The SIT video camera allowed us to record images with fluorescence excitation of sufficiently low intensity that photochemical bleaching of the dye could be avoided for at least 30 min. The video camera output was recorded on magnetic tape and the recorded images were then digitized and stored on a disk of a large computer. Measurements of mitochondrial positions were made from the digitized data. The use of the digitized images made it possible to improve the signal-to-noise ratios (by adding frames and by suppressing background below a certain threshold), and to determine the centroids of the images that were used to define the paths of the mitochondria.

We found that these paths were predominantly random over the experimentally accessible observation times (30 min) and that they satisfied the formal criteria for Brownian motion of a free particle. In a few cases, the motion also showed a slow uniform drift superimposed on the random motion. The mean square displacement per second, which we call the apparent diffusion coefficient, and the apparent drift speed obtained from the analysis are the parameters that quantitatively characterize the motion.

MATERIALS AND METHODS

Cells

Normal rat liver cells, obtained from the American Type Culture Collection, Rockville, MD (ATCC No. CRL 1439), were grown to near confluence (Ham's F12K, 5% CO2, 37° C) on T-75 flasks, trypsinized, and replated at a density of ~40,000 cells on 4 cm × 4 cm glass coverslips submerged in media contained in a petri dish. After overnight culture, the coverslips were mounted in a Corning Bionique chamber (Corning Glass Works, Medfield, MA) and the cells stained with rhodamine 123 (10 μg/ml) as described by Johnson et al. (6).

Optics and Video Techniques

Images of the fluorescent mitochondria were obtained at room temperature with a Leitz Diavert inverted microscope, equipped with epillumination optics and 100 W mercury lamp (E. Leitz, Inc, Rockleigh, NJ). The image of the 100 X objective (NPL Fluotar) was magnified using the 10 x eyepiece (Periplan GFX10M; E. Leitz Co., Rockleigh, NJ) with a

homemade adapter tube and focused onto the photocathode of an SIT video camera (model C1000-12; Hamamatsu Corp., Middlesex, NJ) such that a 120 μm X 100 μm field filled the photocathode as determined by measuring a calibrated 25-μm grating mask (Qualitron Inc, Danbury, CT). The output of the camera was recorded on magnetic tape (model VO5600, Sony Corp, Long Island City, NY). Taped images were digitized using a digital image processor (model DS12/20; Quantex Corp, Houston, TX). Digitized images were stored on the disk of a DEC VAX 11/780 computer and were analyzed using simple FORTRAN programs written for the purpose.

Measurements were carried out as follows. The microscope was focused by viewing the image on the video monitor with the illumination attenuated with neutral density filters as much as possible (typically 100-fold) consistent with seeing an image. The video camera controller (equipped with gain expander) was adjusted for subjectively optimum monitor images. These controls were not adjusted again during an experiment. In our first experiments, we continuously exposed the cells to the illumination (attenuated as above) and the image was recorded continuously. After ~15 min, however, the image started to fade and a diffuse fluorescent background appeared, presumbly because of photochemical reactions of the rhodamine. In subsequent experiments the cells were exposed to the light and the image was recorded for 5 s once every minute. Images could be recorded in this way for as long as 30 min before the diffuse background fluorescence became perceptible. Once the background was observable, we stopped recording the images.

The signal amplitude per pixel within the image of a mitochondrion in a single digitized frame was typically between ~2 and 3 times those of nearby pixels that were not on the mitochondrial image. The low signal-to-noise ratio was caused by the low light levels necessary to avoid photobleaching. To obtain satisfactory images, the Quantex was used to digitize and add 30 consecutive frames. In this way the motion was averaged over 1-s periods, but because the mitochondrial motion occurred in times much slower than 1 s, we did not lose any essential features of the motion.

Differences between image points were calibrated using the image of the aforementioned 25-μm grating mask. With the 100 × objective and the particular combination of eyepiece and photocathode position, a difference of one x-axis pixel and one y-axis pixel corresponded to 0.11 and 0.08 μm, respectively in the center of the field of view. Pincushion distortion caused the grating lines to appear ~10% wider at the edges than at the center of the image. We did not correct for this.

Time base correction for digitizing from the magnetic tape was not necessary. Frame registry was faithful to better than one pixel as determined by digitizing images of static 10–15 μm diameter microspheres. The electronic gain of the video system and the illumination intensity were stable to within 10% for at least 1 h, as determined by monitoring the intensity of the image of fluorescently labeled microspheres.

RESULTS

Images of a single cell with rhodamine-stained mitochondria are shown in Fig. 1, where image 1 *b* was observed 12 min after that in 1 *a*. The nonuniform background, most apparent from left to right in a given photograph, is the result of nonuniform dark output of the SIT video camera. The images shown here are similar to those shown by Johnson et al. (6), who first demonstrated rhodamine 123 staining of mitochondria.

Mitochondrial motion was readily apparent everywhere in the cell, but the mitochondria that were clustered around the nucleus were not suitable for measurements because they moved into the cluster and were lost after only a few minutes. In contrast, in regions away from the edge of the nucleus, the mitochondria were more sparse and individual ones could be picked out and followed for a long time. The mitochondria indicated in Fig. 1 *a* by B1 and B2 are typical of those chosen for study; data for B1 and B2 are presented below.

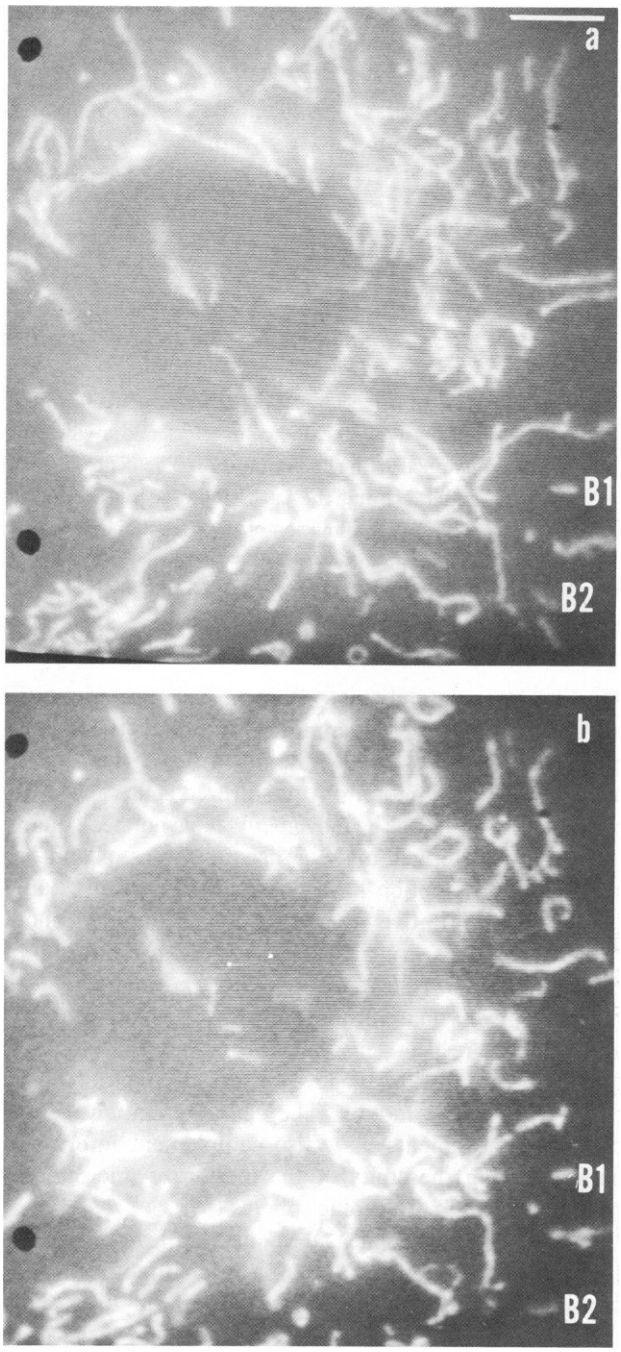

FIGURE 1 Images of rhodamine 123–stained mitochondria. Image in panel *b* was recorded 12 min after that in panel *a*. These are polaroid photographs of the monitor display of the images stored on magnetic tape. Exposure time was 1 s. The mitochondria labeled B1 and B2 were ones represented by the data that are labeled correspondingly in the text and in the tables. The bar represents 5 μm.

Most of the isolated mitochondria appeared as straight or slightly crescent-shaped rods ~1–3 μm long by ~0.2–0.5

μm wide. Some mitochondria fluctuated slowly in shape—between a crescent oriented in one direction and a crescent oriented in the opposite direction. Many of the very long mitochondria and those of complicated shape were actually the superposition of several mitochondria. This was apparent when mitochondria in one image separated into two or more mitochondria in later images. Most of the mitochondria showed concurrent translational and rotational motion, but the rotation was very slow compared with the translation.

We characterized the translational motion of a mitochondrion by following the coordinates of the centroid of its image. The centroid was determined as follows: The image of the cell was displayed on the monitor and a joystick-controlled cursor was positioned at two diagonally opposite corners of a rectangle that enclosed the mitochondrion. The centroid of the intensity distribution for all pixels within the rectangle was calculated using a program written for the purpose. To minimize contributions from background points inside the rectangle, but not on the mitochondrion image, a threshold was subtracted from every pixel. The threshold was specified as an input parameter to the program; it was chosen to be the average intensity of the background as estimated by the intensity of several pixels that were clearly separated from the image of the mitochondrion. The centroid was determined for several values of the threshold, usually within $\pm 20\%$ or so of the average background. The centroid varied by no more than $\pm$ one pixel in X or Y over this threshold range. In the discussion of experimental uncertainties described below, the uncertainty in determining the centroids was taken as $\pm$ one pixel.

The paths followed by the centroids of two mitochondria are shown in Fig. 2. The error bars indicate the $\pm$ one pixel uncertainty (0.11 μm in x and 0.08 μm in y) described above in determining the centroids. The outlines of the two mitochondria are shown at their initial positions. The points in Fig. 2 were obtained at 1-min intervals, but in other experiments we recorded the images continuously (see Materials and Methods), and the motion of the mitochondria appeared to be continuous. In experiments with periodic sampling of the image (as in Fig. 2) we could track a mitochondrion for ~30 min. Thereafter many of the mitochondria meandered into the main cluster or, in some cases, they simply disappeared from view, perhaps by diffusion perpendicular to the image plane.

We attempted to follow mitochondria in six different cell preparations. We were able to obtain tracks suitable for the analysis described below for eight mitochondria from among three cell preparations.

DATA ANALYSIS

The paths followed by the centroids (Fig. 2) resembled those of a classical, two-dimensional Brownian motion (7, 8). The mitochondria selected for detailed study rotated by $\lesssim 20°$ between the first and last observations,

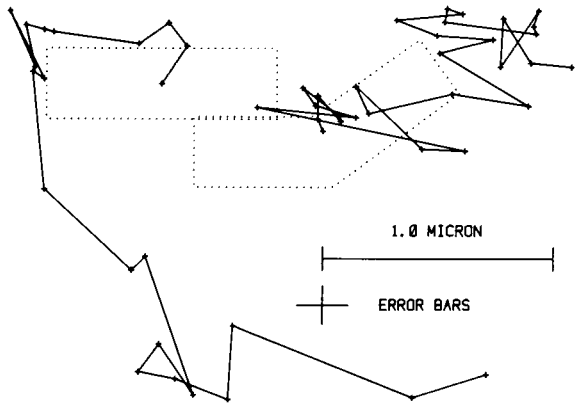

FIGURE 2 The paths followed by the centroids of two mitochondria, each in a different cell. Left and right paths correspond to A1 and B1, respectively, of Table I. The dotted lines are outlines of images at the initial times. For the mitochondrion on the left, the angle that the long axis made with respect to its initial position fluctuated by ~ $\pm 20°$ between the first and last points. The mitochondrion represented by the right-hand path straightened slightly by the last observation, but its overall orientation changed by $<10°$. The small crosses on the paths mark the data points. The error bars (± 0.11 μm in x and ± 0.08 μm in y) are noted in the lower right. The data points are separated by 60-s intervals.

and we therefore neglected rotation in the analysis of the motion. For the analysis, we calculated the parameters that characterize translational Brownian motion and examined whether these calculated parameters were consistent with those of an ideal Brownian motion. For a Brownian random walk, movements along the three Cartesian coordinates are independent of each other and the statistical properties along each coordinate are governed by a Gaussian probability density with zero mean and a mean square displacement that increases linearly in time; that is, the probability that after a time t the particle is found between x_1 and x_2 is (8):

$$p(x_1 < x < x_2 | t) = \frac{1}{\sqrt{4\pi D t}} \int_{x_1}^{x_2} e^{-x^2/4Dt}\, dx, \qquad (1)$$

where the mean square displacement is:

$$\langle x^2 \rangle = 2Dt. \qquad (2)$$

For free diffusion, D is the diffusion coefficient. Motion along the y-direction is described similarly.

The parameters, then, that characterize Brownian motion are the mean displacements and the time dependence of the mean square displacements for each coordinate. We also obtained a crude approximation to the distribution function (Eq. 1) for each coordinate.

Mean Displacements

The mean displacements for x and for y were of the form:

$$\langle x \rangle = \frac{1}{N-1} \sum_{i=2}^{N} (x_i - x_{i-1}), \qquad (3)$$

TABLE I
PARAMETERS OF MITOCHONDRIAL MOTION

I.D. No.*	n‡	$\langle x \rangle$§	$\langle y \rangle$§	D_x‖	D_y‖	$\langle x^2(0) \rangle$¶	$\langle y^2(0) \rangle$¶	V_x**	V_y**
		μm		$10^{-12}\ cm^2 s^{-1}$		$10^{-12}\ cm^2$		$\mu m\ s^{-1}$	
A1	22	0.07 ± 0.04	−0.06 ± 0.02	7.5 ± 0.4	2.5 ± 0.5	0.03	—	~0	1.7×10^{-3}
A2	16	−0.11 ± 0.04	0.01 ± 0.02	6.5 ± 0.3	1.4 ± 0.1	—	0.02	2.1×10^{-3}	~0
A3	22	−0.01 ± 0.04	−0.07 ± 0.02	3.4 ± 0.2	2.2 ± 0.1	—	0.01	1.3×10^{-3}	~0
A4	22	0.04 ± 0.04	−0.03 ± 0.02	5.5 ± 0.6	3.3 ± 0.1	0.08	0.01	~0	~0
B1	29	0.04 ± 0.03	0.01 ± 0.02	1.5 ± 0.1	0.7 ± 0.1	0.05	0.01	~0	~0
B2	29	0.06 ± 0.03	0.05 ± 0.02	3.3 ± 0.3	1.8 ± 0.1	0.14	0.01	~0	~0
C1	14	0.02 ± 0.05	−0.03 ± 0.04	0.5 ± 0.3	0.8 ± 0.2	~0	0.01	~0	~0
C2	9	0.10 ± 0.06	−0.01 ± 0.05	1.3 ± 0.5	0.7 ± 0.3	—	0.01	1.5×10^{-3}	0

*Identification number of mitochondrion. Letters designate different cells, numbers different mitochondria within cell.
‡Number of steps in path.
§Mean displacements.
‖Apparent diffusion coefficients determined from least squares analysis of mean square displacements as function of time (see text).
¶Intercept at $t = 0$ of linear least squares fit to mean square displacements as a function of time.
**Drift speed determined from least squares fit of quadratic function (see text) to mean square displacements as a function of time.

where N is the number of time points and $N - 1$ is the number of time intervals. If the uncertainty in x is σ_x, then the uncertainty in the difference between two x-coordinates is $\sqrt{2}\,\sigma_x$ (9). The uncertainty in the mean x-displacement is $\sqrt{2}\,\sigma_x/\sqrt{N-1}$. The uncertainty in the mean y-displacement is of the same form with σ_y instead of σ_x. The uncertainties σ_x and σ_y were ± 0.11 and 0.08 μm for x and y, respectively. The mean displacements are listed in Table I.

Mean Square Displacements

For a Brownian motion, the time intervals are statistically independent. If the paths are sampled at period t, and if the mean square displacement in this interval is $\langle x^2(t) \rangle$, then the mean square displacement over a period nt is

$$\langle x^2(nt) \rangle = n \langle x^2(t) \rangle. \tag{4}$$

For a set of experimental data with N points sampled at period t, there are $N - 1$ intervals of length t; $N - 2$ intervals of length $2t$, etc. If the motion is Brownian, then the mean square displacements should be proportional to the elapsed time with a proportionality coefficient of $2D$ (Eq. 2).

Fig. 3 shows plots of mean square displacements calculated for the two paths displayed in Fig. 2. The uncertainty in the mean square displacements over any time interval is (9):

$$\sigma_{\langle x^2 \rangle} = \sqrt{2}\,\langle x^2 \rangle / \sqrt{n},$$

where n is the number of intervals in the calculation of the mean square displacements. The straight lines shown for x (Fig. 3 *a*) and x and y (Fig. 3 *b*) are the least squares best fit to the data. The plots for y (Fig. 3 *a*), and for several other cases not shown, were clearly not linear. We attributed the nonlinearity to the presence of uniform motion (drift) in addition to the Brownian motion. In this case, the mean square displacement is:

$$\langle x^2(t) \rangle = 2Dt + v^2 t^2, \tag{5}$$

where v is the drift speed. The quadratic function (Eq. 5) can be fit to the data by carrying out a linear least squares fit to $\langle x^2 \rangle / t$. The curve shown in Fig. 3 *a* shows the fit of the data to this quadratic function.

In several cases, such as the x-coordinate in Fig. 3 *b*, the data fit a straight line very well (pairwise correlation coefficient >0.97), but the line did not pass through the

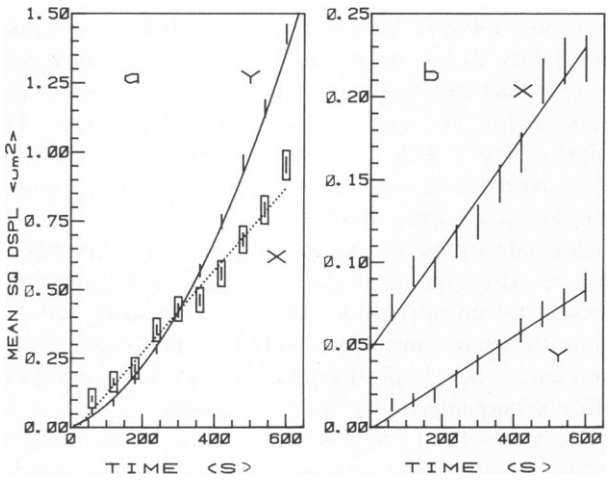

FIGURE 3 Mean square displacements as a function of time for paths shown in Fig. 2. Panels *a* and *b* here correspond to the left and right paths, respectively, in Fig. 2. *X* and *Y* labels refer to data sets for the respective coordinates. Rectangles enclosing data points in *a* are to help distinguish *X* and *Y* points from each other. Error bars are described in the text. Straight lines are least squares best fit to the midpoints of the error bars. Curved solid line in panel *a* is least squares best fit of quadratic function (Eq. 5, text). Parameters are listed in Table I, in which A1 refers to panel *a* and B1 to panel *b*.

origin as it ought to for a Brownian motion. The positive intercept at $t = 0$ means that the motion had a component for which the mean square displacement was independent of time. One type of random motion for which the mean square displacement is independent of time is that of a randomly driven harmonic oscillator (8). This type of motion may be manifested in the analysis of the mitochondrial movements because the mitochondria change shape. We noticed that all of the plots with positive intercepts corresponded to mitochondria that changed over the observation period from a crescent oriented in one way to a crescent oriented oppositely. These shape changes of the mitochondria were reminiscent of the shape changes associated with thermal fluctuations of large cylindrical, elastic phospholipid vesicles studied by Schneider et al. (10). The random shape changes of these vesicles could be described in terms of randomly driven normal mode harmonic oscillators. Thus, if the shape changes of the mitochondria correspond to normal deformation modes of an elastic body, then the mean square displacements of the centroids of the mitochondria would have a time independent term caused by the shape changes. The net displacement due to translation and shape change together is $x = x_t + x_s$, where x_t and x_s are the displacements due to translation and shape change, respectively. The mean square displacement is:

$$\langle x^2(t) \rangle = \langle x_t^2 \rangle + \langle x_s^2 \rangle + 2\langle x_t x_s \rangle.$$

If the shape change and translation motion are independent, then $\langle x_t x_s \rangle = 0$ and $\langle x_s^2 \rangle$ is the intercept of the plot of $\langle x^2(t) \rangle$ vs. t.

The data were not sufficient to support a detailed analysis of the shape changes, but the magnitudes estimated for the displacements of the centroids caused by shape changes appeared to be consistent with the magnitudes of the intercepts. For example, when the shape changed from a crescent oriented in one direction to its mirror image position, the centroid shift (with respect to the center of the axis along the mitochondrion) was of magnitude 0.1 μm. The intercepts observed from the plots such as Fig. 3 *b* (x-coordinate) were in the range 0.01–0.14 μm^2 (Table I). We did not attempt to analyze the time dependence of the mean square displacements simultaneously for the linear and quadratic coefficients and the intercept. We intended only to explain the main characteristics of the data, rather than to carry out detailed fits of curves to the data.

The foregoing experimental and analytical methods were checked by recording and analyzing tracks of fluorescently labeled polystyrene spheres (0.85 μm diam, Polysciences, Inc., Warrington, PA) suspended in water in the same chambers used to hold the cells. The diffusion coefficient obtained from the analysis of the images as described above was 5.4×10^{-9} cm^2 s^{-1}; that calculated from the Stokes-Einstein equation ($D = kT/6\pi\eta R$) was 4.7×10^{-9} cm^2 s^{-1}.

Table I lists the apparent diffusion coefficients and the drift speed inferred from the least squares linear or quadratic fit, as appropriate to the mean square displacement data. The uncertainties are the standard errors in the slopes calculated in the least squares analysis. The letters refer to one cell; thus A1–A4 were for mitochondria in one cell; B1 and B2 in another.

Probability Density

There were two mitochondria that did not drift and yielded enough data to obtain a crude approximation to the distribution function. This was accomplished for the x- and y-coordinates of the two paths by counting the number, n, of steps that had lengths between 1 and 1 + d1, where d1 was 0.1 μm, and expressing the data as the fraction, n/N, for each interval, where N was the total number of observed steps. The corresponding distribution expected from Eq. 1 was calculated by evaluating the integral of Eq. 1 with the variance determined from the slope of the least squares straight lines fit to the mean square displacements as a function of time. These calculated values are listed in Table II, along with those observed for the two mitochondria. In Table II, the experimental data are listed separately for positive and negative displacements, and are indicated by the positive and negative signs at the head of the columns. The theoretical distribution function is symmetric and only a single column of data is listed for the calculated values. The agreement is fairly good, considering the small number of experimental data points.

TABLE II
STEP SIZE DISTRIBUTION FUNCTION

I.D. No.*	d‡	P_x(cal)§	P_x(obs)§		P_y(cal)§	P_y(obs)§	
			+	−		+	−
	μm						
B1	0–0.10	0.27	0.28	0.15	0.36	0.48	0.22
	0.10–0.20	0.16	0.16	0.15	0.13	0.04	0.15
	0.20–0.30	0.06	0.07	0.07	0.01	0.07	0.04
	>0.30	0.01	0.07	0.07	0	0	0
B2	0–0.10	0.19	0.24	0.20	0.25	0.32	0.32
	0.10–0.20	0.15	0.20	0.08	0.16	0.16	0.12
	0.20–0.30	0.09	0.08	0.08	0.07	0.04	0
	0.30–0.40	0.04	0	0	0.02	0	0
	>0.40	0.03	0.08	0	0	0	0

*Identification number of mitochondrion. Same notation as in Table I.
‡Displacement interval.
§P is the fraction of the total number of steps that have length between the intervals in the first column.

$$P(\text{cal}) = \frac{1}{\sqrt{4\pi Dt}} \int_{x_1}^{x_2} e^{-x^2/4Dt}\, dx,$$

where values of D are listed in Table I. P(obs) is n_i/N, where $N = 29$ and is the total number of experimentally observed steps and n_i is the number of steps of length between the intervals in the first column. Columns headed + and − refer to the sign of the displacements. Calculated values are symmetric about origin.

DISCUSSION

The foregoing data show that the movements of the mitochondria in these cells under the particular observation conditions were dominated by random movements that satisfied the criteria for Brownian motion of a free particle, namely, the mean square displacements increased linearly with time, the mean displacements were zero, and the histograms approximating the probability distribution were consistent with the expected Gaussian distribution function. In several cases a slow drift of unknown cause was superimposed on the random process.

The random movements of the mitochondria described herein are in contrast to observations made long ago (2), in which mitochondria were reported to move along defined paths. Random motion would also be expected to be a minor contribution to organelle motion in cells within which there is cytoplasmic flow. We do not know of any quantitative study of the latter case. We assume, however, that intracellular organelle motion can differ qualitatively and quantitatively among cell types and under different observation conditions. For the cells studied herein, over the time intervals reported, the predominant mitochondrial movements are unambiguously random. The driving forces of the motion remain to be established. The study here shows that the random motion can be parameterized, and that the motion is amenable to a more detailed quantitative study.

In every case, the parameters deduced for x and y coordinates of a mitochondrion were not equal to each other. This asymmetry may simply reflect the rod-like shape of the mitochondria, which was not averaged out because the rotation was slow. The direction closest to the normal to the long axis of the mitochondria was the direction of lowest diffusional mobility. It so happened that most of the mitochondria selected for measurements were oriented with their long axes pointed roughly in the x-direction. We did not, however, attempt to analyze the asymmetry quantitatively.

We note that the effective diffusion coefficients vary several-fold among different mitochondria within the same cell. These differences may reflect a combination of inhomogeneity in the cytoplasm and the sizes of the mitochondria. Even though these differences are well outside of the formal quoted uncertainties of the measurements, we do not feel that the data are sufficient to allow us to suggest a detailed interpretation of these differences.

The magnitudes of the effective translational diffusion coefficients for all of the mitochondria were in the range of 10^{-11}–10^{-12} cm^2 s^{-1}. The diffusion coefficient of a sphere of diameter 2 μm in water calculated from the Stokes-Einstein relationship is $\sim 3 \times 10^{-9}$ cm^2 s^{-1}. Thus if the mitochondria were undergoing diffusion, in the strict sense of the word, then the effective viscosity of the cytoplasm would exceed 70 cp (i.e., greater than that of 60% sucrose). In view of what is now known about the cytoskeleton, it is an oversimplification to describe the cytoplasm as a high viscosity liquid. Nevertheless, the resistance to motion, as expressed by an effective viscosity for the mitochondria, is consistent with the ~70 cp estimated by Wojcieszyn et al. (4) from a study of diffusion of fluorescently labeled bovine serum albumin microinjected into cells.

The experiments herein demonstrate that motion of at least some mitochondria can be quantitatively characterized. The spatial distribution, however, of mitochondria in the cell is not uniform and the structures that maintain the nonuniformity, especially the high density around the nucleus, are not known. Thus it remains to be seen whether the isolated mitochondria, upon which the present measurements were made, are typical of all of the mitochondria in the cell. In addition, it remains to be seen whether the parameters differ among cell types, whether they respond to colchicine or other chemical perturbations, or whether they differ at various stages in the cell cycle.

REFERENCES

1. Frederic, J. 1954. Action of various substances on the mitochondria of living cells cultivated in vitro. *Ann. NY Acad. Sci.* 58:1246–1263.
2. Gey, G. O., P. Shapras, and E. Borysko. 1954. Activities and responses of living cells and their components as recorded by cinephase microscopy and electron microscopy. *Ann. NY Acad. Sci.* 58:1089–1109.
3. Ernster, L., and G. Schatz. 1981. Mitochondria: a historical review. *J. Cell Biol.* 91 (Suppl.):227s–255s.
4. Wojcieszyn, J. W., R. A. Schlegel, E-S. Wu, and K. A. Jacobson. 1981. Diffusion of injected macromolecules within the cytoplasm of living cells. *Proc. Natl. Acad. Sci. USA.* 78:4407–4410.
5. Beckerle, M. C. 1984. Microinjected fluorescent polystyrene beads exhibit saltatory motion in tissue culture cells. *J. Cell Biol.* 98:2126–2132.
6. Johnson, L. V., M. L. Walsh, and L. B. Chen. 1980. Localization of mitochondria in living cells with rhodamine 123. *Proc. Natl. Acad. Sci. USA.* 77:990–994.
7. Chandrasekhar, S. 1943. Stochastic problems in physics and astronomy. *Rev. Mod. Phys.* 15:1–89.
8. Papoulis, A. 1965. Probability, Random Variables, and Stochastic Processes. McGraw-Hill Book Co., Inc. New York. 524–528.
9. Baird, D. C. 1962. Experimentation: An Introduction to Measurement Theory and Experimental Design. Prentice-Hall, Inc. Englewood Cliffs, NJ. 48–74.
10. Schneider, M. B., J. T. Jenkins, and W. W. Webb. 1984. Thermal fluctuations of large cylindrical phosopholipid vesicles. *Biophys. J.* 45:891–899.